Websites:
http://www.nbmedicine.org
http://www.sciencepub.net/nurse

Emails:
editor@sciencepub.net
nbmeditor@gmail.com

Biomedicine and Nursing

MARSLAND PRESS
Multidisciplinary Academic Journal Publisher

3-Dimensional Analytical Solution for Lunar Descent Scheme

Ibrahim Mustafa Mehedi [1], Takashi Kubota [2], Ubaid M Al-Saggaf [1]

[1.] Department of ECE, Faculty of Engineering, King Abdulaziz University, Jeddah 21589, Saudi Arabia
[2.] The University of Tokyo, Tokyo, Japan
imehedi@kau.edu.sa

Abstract: Lunar and Mars landing is a crucial part of any exploration mission. Its importance is manifested by the considerable interest in the past couple of decades. Solution of lunar descent can be either numerical or analytical. Numerical solutions are iterative and computationally demanding and some of them might not be suitable for on-board implementation. On the other hand, analytical solutions are not complex and much more attractive for the same purposes. All the present analytical solutions schemes are two dimensional considering only altitude and down range to describe the reference trajectories of a lunar descent. The main contribution of this paper is the development of a complete 3-dimensional analytical solution for the reference trajectory which is crucial for a precise landing of a lunar spacecraft. Comparisons are made by simulated responses between numerical and analytical solutions. Detail mathematical derivations are presented in this paper as well.
[Ibrahim MM, Takashi K, Ubaid MS. **3-Dimensional Analytical Solution for Lunar Descent Scheme**. *Biomedicine and Nursing* 2022;8(1):17-25]. ISSN 2379-8211 (print); ISSN 2379-8203 (online). http://www.nbmedicine.org 3. doi:10.7537/marsbnj080122.03.

Keywords: Lunar descent; Numerical solution; Analytical solution; 3-D modeling

1. Introduction

Lunar and Mars landing is a crucial part of any exploration mission. Its importance is manifested by the considerable interest in the past couple of decades [1-9]. For a lunar lander, it is essential that the landing on the lunar surface is vertical and soft. A scheme to fulfill this requirement is the gravity-turn descent that has been used for both lunar and Mars probes [1, 2, 10-13]. In this descent technique, the lander thrust vector is maintained opposite to the instantaneous velocity vector along the descent path [14]. The great benefit of gravity-turn descent is that the landing is assured to be vertical and the guidance law is close to fuel optimum [3]

Lunar guidance takes a horizontally oriented spacecraft from orbital speeds, hundreds of kilometers from the desired landing point, to a very low speed and an almost vertical orientation. Guidance schemes for lunar landing date back to the Apollo era [4, 5]. The Apollo lunar descent guidance schemes worked well to meet the criteria of the 1960s. However, they cannot fulfill the demanding goals of future lunar exploration that encompasses the desire to easily and cheaply explore several locations on the moon.

In conventional gravity-turn descent guidance law, the solution of spacecraft equations of motion is numerical and iterative. Due to complexity, a numerical solution limits real time implementation. Therefore, it is impartial to seek an analytical solution. An analytical targeting solution can generate multi-dimensional trajectories on-the-fly and easily re-target the spacecraft to another landing site. At the end of the last century, a 2-dimensional analytical solution was developed for lunar landing mission [14] and [3]. The same 2-dimensional concept is proposed in [15] based on an analytical solutions to the equations for down range and altitude but excluding cross range distance. However, in the literature and up to date there is no result for a full analytical 3-dimensional spacecraft reference trajectory that includes cross range, altitude and down range distance. This gap in the literature is filled by the present paper. The main contribution of this paper is the development of a complete 3-dimensional analytical solution for the reference trajectory which is crucial for a precise landing of a lunar spacecraft.

An advantage of numerical solutions is the ability to accommodate constraints in the state and control variables inherent in planetary landing optimal control problems. This advantage is offset by the fact that numerical solutions are iterative, computationally expensive and not suitable for on-board implementation. Nevertheless, some authors proposed solving an on-board nonlinear optimization problem [16]. Other authors tried to overcome the computational burden by solving a related problem that does not minimize fuel use [17]. However, the applicability of nonlinear optimization approaches to on-board implementation is limited. This is due to the

fact that with such techniques it is not possible to a have a priori knowledge of the required number of iteration needed to find a feasible trajectory and there is no guarantee of achieving the global optimum. Nevertheless, recent advances in convex optimization may remedy the problem. The applicability of such techniques for on-board implementation made feasible by advances in computing power, modern algorithms and new coding techniques that exploits the structure of the given problem [18]. One of these approaches is described in [19] where approximate solutions to the minimum-fuel powered-descent guidance are formulated as a second order cone program (SOCP). This optimization problem can be solved in polynomial time using interior-point-method algorithms [20-22]. For any given accuracy, the global optimum can be found with a priori upper bound on the required number of iteration needed to achieve the optimum. The limitation of the approach in [19] is that it assumes a feasible solution exists. This limitation is eliminated in [12] to handle the case when there is no feasible trajectory to the target exists. This approach is extended even further in [23] where lossless convexifications are used when the problem has non-convex control constraints. Extensive comparisons of the convex optimization approach to alternative approaches are given in [12, 23, 24]. One last remark is that advances in computing power are not quickly implemented in the very expensive space hardened microprocessors. The state of the art on-board processor is still the RAD750TM space hardened microprocessor [25, 26] that is identical in architecture, function, and operation to the commercial IBM PowerPC750TM microprocessor. It is only 400 Dhrystone 2.1 MIPS at 200 MHz which far behind in performance when compared with the present desktop microprocessors.

This paper is structured as follows. Section 2 describes the 3-dimensional equation of motion for a spacecraft lunar descent including the used preliminary postulation. 3-dimensional numerical solutions are presented in Section 3. 3-dimensional analytical solutions to the equations for speed, time, vertical range, downrange, and cross range distance as a function of velocity vector pitch angle are presented in Section 4. Descent parameter specifications used in the simulation are mentioned at the end of this Section as well. Simulation results are shown in Section 5 for both numerical and analytical solutions. Section 6 represents a complete comparison of the analytical and numerical solutions for the 3-dimensional trajectory responses for spacecraft descent on a lunar surface. Finally Section 7 contains the conclusion.

2. 3-Dimensional state equations

A lunar descent schematic diagram is shown in Figure 1 where the local vertical local horizontal (LVLH) reference frame is denoted by L. The figure also shows the relationship of the maneuver frame, denoted by M ,to the LVLH unit vectors.

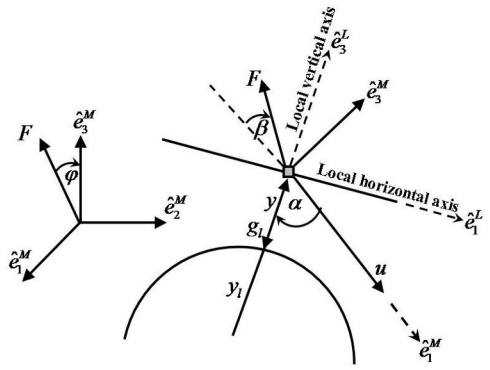

Figure 1. Schematic diagram of lunar descent

The fundamental three dimensional equations of motion describing a spacecraft landing on a uniform sphere-shaped lunar body [1] are divided into two parts. The first part describes the spacecraft dynamics and is given by the following equations:

$$\dot{u}(t) = g_l \cos\alpha - N\cos\beta \tag{1}$$

$$\dot{\alpha}(t) = \frac{1}{u}[(\frac{u^2}{y+y_l} - g_l)\sin\alpha - N\sin\beta\cos\phi] \tag{2}$$

$$\dot{\psi}(t) = \frac{1}{u\sin\alpha}[N\sin\beta\cos\phi] \tag{3}$$

Where u is the magnitude of the spacecraft velocity vector, g_l is the lunar gravitational acceleration, N is the ratio of thrust F to the vehicle mass m, α is the pitch angle of the vehicle velocity vector relative to the local vertical, β is the thrust vector angle relative to the opposite of the velocity vector, y is the altitude of the spacecraft from lunar surface, yl is the lunar radius, ψ is the cross range angle and ϕ is the thrust roll angle.

The second part describes the kinematics and is given by the following equations:

$$\dot{y}(t) = -u\cos\alpha \tag{4}$$

$$\dot{x}(t) = u\sin\alpha\cos\psi\frac{y_l}{y+y_l} \tag{5}$$

$$\dot{c}(t) = u\sin\alpha\sin\psi\frac{y_l}{y+y_l} \tag{6}$$

where x and c are the horizontal span and cross range distance.

2.1. Preliminary postulation

The right hand sides of the spacecraft governing equations are reduced to functions of the velocity vector pitch angle α. To do this we make some reasonable assumptions regarding thrust to mass ratio, thrust vector angle and lunar gravitational acceleration force. To generate an ideal descent trajectory, it is rational to assume constant values for N (i.e., F/m) and g_l and to set β to zero. These are not restricting assumptions since in the case of constant thrust acceleration, m will not be constant and thus F/m will be varying but the error will be removed by the real time guidance algorithm. With these assumptions, equations (1) to (3) reduce to:

$$\dot{\alpha}(t) = \frac{1}{u}[(\frac{u^2}{y + y_l} - g_l)\sin\alpha] \tag{7}$$

$$\dot{u}(t) = g_l \cos\alpha - N \tag{8}$$

and

$$\dot{\psi}(t) = 0 \tag{9}$$

Therefore, ψ (t) is constant. Since landing must take place close to the lunar surface, consequently it is a reasonable practical assumption that $y << y_l$ which implies that $y_l / y + y_l \approx 1$. Using this in equations (5) and (6) gives:

$$\dot{x}(t) = u\sin\alpha\cos\psi \tag{10}$$

$$\dot{c}(t) = u\sin\alpha\sin\psi \tag{11}$$

3. 3-D numerical solution

To find a numerical solution during the powered descend phase, the above equations need to be simplified and rearranged in a format suitable for a numerical solver. We derive below the equations for speed u, time t, down-range x, altitude y and cross range c as a function of a single variable; namely the velocity vector pitch angle α. Using equations (7) and (8), the equation for speed u is derived as follows:

$$\dot{u}(\alpha) = \frac{du}{dt} \Big/ \frac{d\alpha}{dt} = \frac{u(g_l\cos\alpha - N)}{(u^2 / y_l - g_l)\sin\alpha} \tag{12}$$

then

$$\frac{1}{u}(\frac{u^2}{y_l} - g_l)du = \frac{g_l\cos\alpha - N}{\sin\alpha}d\alpha$$

This can be integrated as:

$$\int_{u_0}^{u}\frac{1}{u}(\frac{u^2}{y_l} - g_l)du = \int_{\alpha_0}^{\alpha}\frac{g_l\cos\alpha - N}{\sin\alpha}d\alpha$$

Therefore, the equation for speed becomes

$$u(\alpha) = [-g_l y_l W]^{\frac{1}{2}} \tag{13}$$

where the Lambert W function is expressed as:

$$W = -\frac{u_0^2}{g_l y_l}\frac{\sin\alpha^{-2}}{e^{(\frac{u_0^2}{g_l y_l})}}\left(\frac{1+\cos\alpha}{\sin\alpha}\right)^{-\frac{2N}{g_l}} \tag{14}$$

Using equations (8) and (12), the descent time tD can be obtained by integrating the following equation expressed as a function of α:

$$\dot{t}_D(\alpha) = \frac{dt_D}{d\alpha} = \frac{du}{d\alpha} \Big/ \frac{du}{dt_D} = \frac{\dot{u}(\alpha)}{\dot{u}(t)} \tag{15}$$

Similarly, the equation for altitude can be rewritten as:

$$\dot{y}(\alpha) = \frac{dy}{d\alpha} = \frac{dy}{dt_D}\frac{dt_D}{d\alpha} = \dot{y}(t)\dot{t}_D(\alpha) \tag{16}$$

Now substituting the values from equation (4) gives:

$$\dot{y}(\alpha) = -u\cos(\alpha)\dot{t}_D(\alpha) \tag{17}$$

where u can be replaced from equation (13). Similar procedure can be followed to express the horizontal span as a function of the velocity vector pitch angle α.

$$\dot{x}(\alpha) = \frac{dx}{d\alpha} = \frac{dx}{dt_D}\frac{dt_D}{d\alpha} = \dot{x}(t)\dot{t}_D(\alpha) \tag{18}$$

Using equation (10) gives:

$$\dot{x}(\alpha) = u\sin\alpha\cos\psi\dot{t}_D(\alpha) \tag{19}$$

A similar procedure is applied to derive the following equation for the cross range:

$$\dot{c}(\alpha) = u\sin\alpha\sin\psi\dot{t}_D(\alpha) \tag{20}$$

4. 3-D analytical descent solution

Here we derive a 3-dimensional full analytical solution for the lunar descent problem. We make the reasonable practical assumption that the lunar surface for this problem can be considered as a plane surface. That is yl → ∞ so that equation (7) now reduces to:

$$\dot{\alpha}(t) = -\frac{g_l}{u}\sin\alpha \tag{21}$$

This reduced equation is used to obtain a single, distinguishable differential equation with α as the self-regulating variable. From the above we have:

$$\dot{u}(\alpha) = \dot{u}(t)/\dot{\alpha}(t) = -\frac{u(g_l\cos\alpha - N)}{g_l\sin\alpha} \tag{22}$$

then

$$\frac{1}{u}\frac{du}{d\alpha} + \frac{\cos\alpha}{\sin\alpha} - \frac{N}{g_l}\frac{1}{\sin\alpha} = 0 \tag{23}$$

Now Eq. (23) can be integrated to obtain the descent speed u as a function of velocity vector pitch angle α as [1,3]:

$$u(\alpha) = u_0\left[\frac{\sin\alpha_0}{\sin\alpha}\right]\left[\frac{\tan(\alpha/2)}{\tan(\alpha_0/2)}\right]^{\frac{N}{g_l}} \quad (24)$$

where, u0 and α0 are initial values for speed and velocity vector pitch angle respectively.
Differentiating Eq. (24):

$$\dot{u}(\alpha) = \frac{du}{d\alpha} = u_0\left[\frac{\sin\alpha_0}{\sin\alpha}\right]\left[\frac{\tan(\alpha/2)}{\tan(\alpha_0/2)}\right]^{\frac{N}{g_l}}\left[\frac{N}{g_l\sin(\alpha)} - \cot\alpha\right] \quad (25)$$

Using the above value of the speed u, we can obtain the solution for time, altitude, down range and cross range. First, the descent time is given as:

$$\dot{t}_D(\alpha) = \frac{dt_D}{d\alpha} = \frac{du}{d\alpha}\Big/\frac{du}{dt_D} \quad (26)$$

Using equations (8) and (25) gives:

$$\dot{t}_D(\alpha) = u_0\left[\frac{\sin\alpha_0}{\sin\alpha}\right]\left[\frac{\tan(\alpha/2)}{\tan(\alpha_0/2)}\right]^{\frac{N}{g_l}}\left[\frac{N}{g_l\sin(\alpha)} - \cot\alpha\right]\left[\frac{1}{g_l\cos\alpha - N}\right] \quad (27)$$

Similarly, the altitude is given as:

$$\dot{y}(\alpha) = \frac{dy}{d\alpha} = \frac{dy}{dt_D}\Big/\frac{d\alpha}{dt_D} \quad (28)$$

Using equations (4), (21) and (25) gives:

$$\dot{y}(\alpha) = \frac{u^2}{g_l}\cot\alpha = u_0^2\left[\frac{\sin\alpha_0}{\sin\alpha}\right]^2\left[\frac{\tan(\alpha/2)}{\tan(\alpha_0/2)}\right]^{\frac{2N}{g_l}}\left[\frac{\cot\alpha}{g_l}\right] \quad (29)$$

Using equations (10) and (21), the down range distance is given as:

$$\dot{x}(\alpha) = \frac{dx}{dt_D}\Big/\frac{d\alpha}{dt_D} = -\frac{u^2}{g_l}\cos\psi \quad (30)$$

Using equations (25) gives:

$$\dot{x}(\alpha) = -u_0^2\left[\frac{\sin\alpha_0}{\sin\alpha}\right]^2\left[\frac{\tan(\alpha/2)}{\tan(\alpha_0/2)}\right]^{\frac{2N}{g_l}}\left[\frac{1}{g_l}\right]\cos\psi \quad (31)$$

Similarly, using equations (11) and (21), the cross range distance is given as:

$$\dot{c}(\alpha) = \frac{dc}{dt_D}\Big/\frac{d\alpha}{dt_D} = -\frac{u^2}{g_l}\sin\psi \quad (32)$$

Using equations (25) gives:

$$\dot{c}(\alpha) = -u_0^2\left[\frac{\sin\alpha_0}{\sin\alpha}\right]^2\left[\frac{\tan(\alpha/2)}{\tan(\alpha_0/2)}\right]^{\frac{2N}{g_l}}\left[\frac{1}{g_l}\right]\sin\psi \quad (33)$$

4.1. Descent constraints

To compare the analytical and numerical solutions, parameters have to be specified. These specifications are shown in Table 1.

Table 1. Lunar descent specification

Lunar descent specification	
Lunar gravitational acceleration (gl)	1.623 [m/s 2]
Thrust to mass ratio (N)	4 [N/kg]
Initial lander speed (u0)	1688 [m/s]
Initial velocity vector pitch angle (α0)	90 [deg]
Initial altitude for powered descent	100 [km]

5. Simulation results

As can be seen from the previously derived equations, the cross range angle ψ has no effect on speeds, time and altitude. As such, the trajectory responses for descent speeds, time and altitude are plotted in Figure 2 as function of the velocity vector pitch angle α. For comparison, both the analytical and the numerical solutions are shown. The full integrated numerical solution is considered as an ideal solution and a benchmark for lunar descent trajectory and it is used to evaluate any other solution. However, it is to be noted that this method is complex, iterative and needs a long time to execute and thus not suitable for real time precise landing application. We will demonstrate that our analytical solution is close to this ideal numerical solution.

From Figure 2, speed and time responses for both the numerical and analytical solution are almost similar. However, there is a deference in the altitude response as shown in Figure 2(d). From the figure, as the velocity vector pitch angle approaches zero, the analytical solution, reaches closer to the surface than that of the numerical solution. This means that the analytical solution takes the spacecraft at lower altitude to initiate terminal descent.

One of the contributions of this paper is the emphasis of non-zero cross range angle for precise lunar landing which was overlooked in the past. Cross range angle is a major factor influencing the cross range distance. A simulation is performed for both the numerical and the analytical solutions where the cross range angle is varied to show its impact on the cross range distance. It is observed that when the

cross range angle is maintained at zero degree, the lunar landing spacecraft does not perform any cross range travel. When the cross range angle is varied between 0 and 25 degrees, the cross range travel is more than 150 [km]. When the cross range angle is varied between 0 and 5 degrees, the cross range travel is within 32.5 [km]. Similarly when the cross range angle is varied between 0 and 0.5 degrees, the cross range travel is more than 3 [km]. Figure 3 shows some sample plots.

The cross range angle is an important factor for precise lunar landing mission. In previous investigations, 2-D lunar descent trajectories are designed considering only the altitude and down range distance. In these investigations, the assumption of zero cross range angle is made [3,15,27]. With such assumption, the cross range travel will be zero. Thus the important cross range distance parameter is overlooked. But as can be seen from figure 3, the trajectory is very sensitive to the cross range angle. A small cross range angle of 0.1 degrees can result in more than 600 m cross range travel and if the angle is 0.5 degrees, the landing spacecraft moves more than 3 [km] from the line of down range.

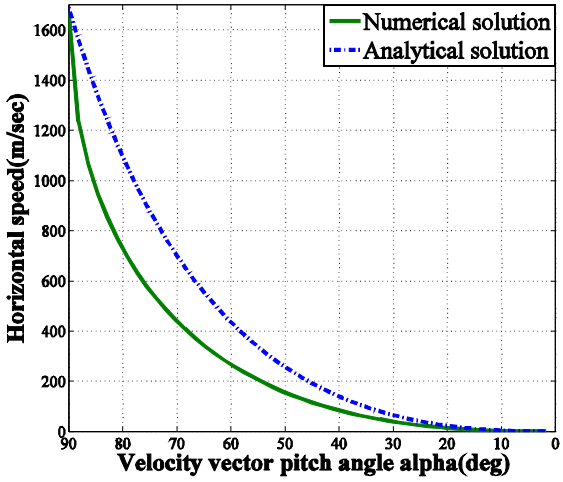

(a) Horizontal speed

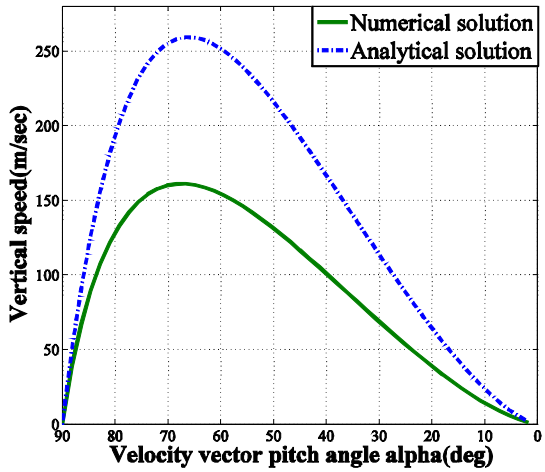

(b) Vertical speed

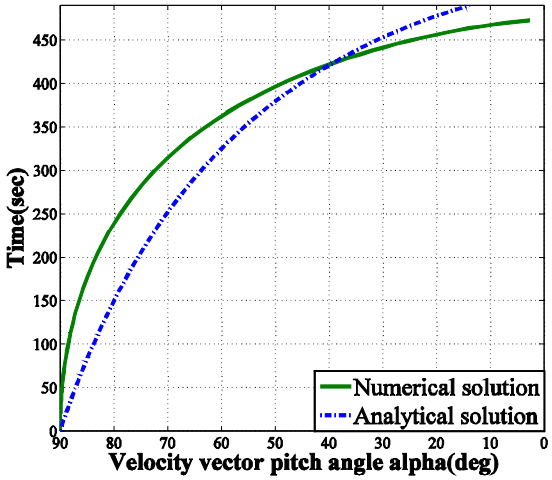

(c) Time

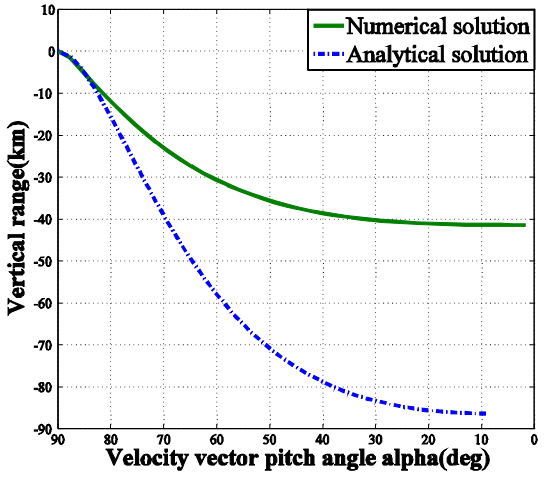

(d) Altitude

Figure 2. Comparison of numerical solution to analytical solution: Speed, Time and Altitude

The above analysis proves that the 3-D analysis, including cross range angle, is instrumental in trajectory design for precise lunar landing missions which was absent in conventional 2-D trajectory designs. Moreover, it is not only the cross range distance that is affected by changes of the cross range

angle. The down range distance is also influenced. Figures 4 shows the simulation results for down range response of both numerical and analytical solutions as a function of velocity vector pitch angle α. The figure shows that an increase in the cross range angle will result in a decrease of the down range distance. As a result, the lunar landing spacecraft will travel a shorter distance than required. A cross range angle increase of up to 25 degrees will result in down range distance decreases of more than 30 [km] as shown in Figure 4.

It is already mentioned that the analytical solutions are introduced to reduce the complexity of the numerical solution. The above simulation results for cross range and down range responses show that there is only a very small deviation between the numerical and analytical solutions. The analytical solution of lunar descent motion equation is much more suitable for real-time precise landing application and the small errors of cross range and down range can be eliminated by using real-time guidance scheme during the descent.

6. 3-Dimensional response

Section 3 and 4 described a detailed 3-dimensional mathematical modeling of a lunar landing mission. Numerical and analytical solutions are derived and a computer simulation is performed.

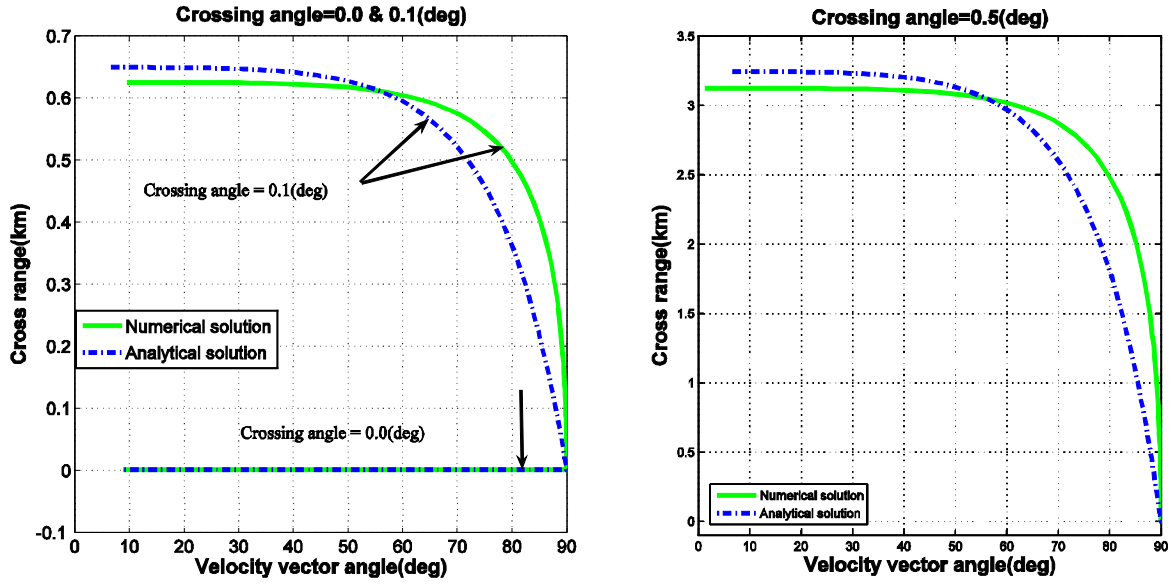

Figure 3. Cross range response

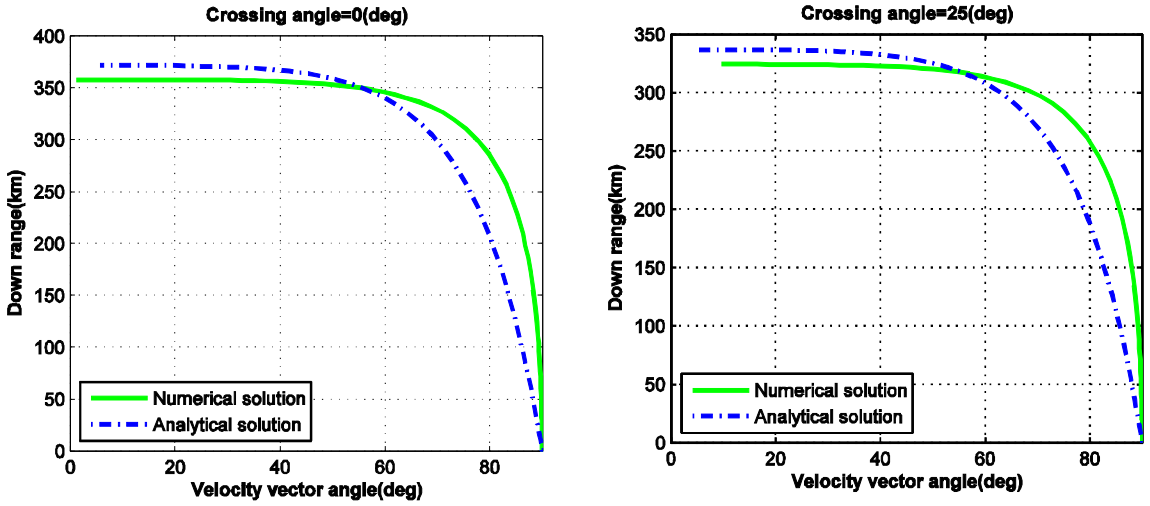

Figure 4. Down range response

Figure 5 shows the trajectories for both the numerical and analytical solutions. In the simulation, the constant values shown in Table 1 are used for lunar gravitational acceleration g_l, thrust to mass ratio N, initial vehicle speed $u_0$and initial velocity vector pitch angle α_0. Simulation is performed for deferent values of cross range angle. It is observed that altitude is not affected at all by changing the cross range angle. On the other hand, down range and cross range distances are affected by changes in the values of cross range angle.

The simulation shows that the trajectories of the less complex analytical solution are always following the response of ideal but complex numerical solution. As shown in Figure 5, the altitude of analytical solution is maintained 40 km lower than the numerical solution. This low altitude flight path may assist the lunar landing spacecraft to activate terrain based navigation devices for hazard avoidance and safe landing.

Table 2. Elapse time comparison using laboratory desktop computing [second].

Numerical solution	3D analytical solution
4.22	0.03

Table 3. Simulated elapse time comparisons for on-board computer [second].

Numerical solution	3D analytical solution
56.25	0.40

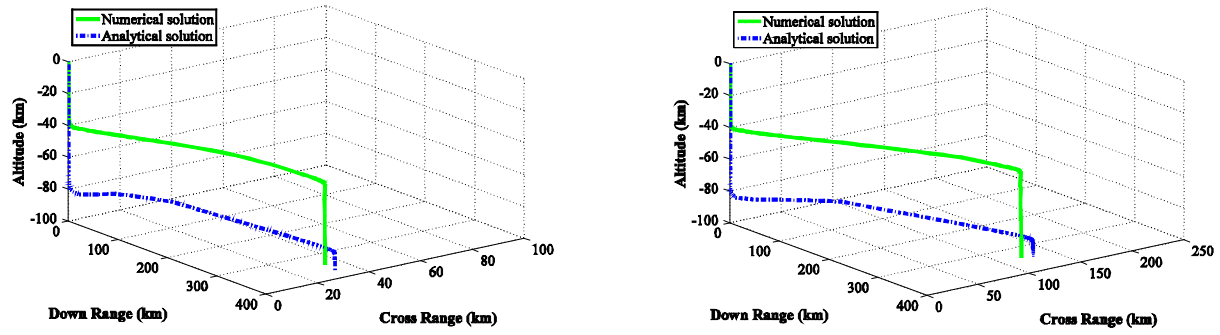

(a) Crossing angle = 5 degree (b) Crossing angle = 20 degree

Figure 5. 3-dimensional flight path comparison between numerical and analytical solution for deferent crossing angle

To better understand the complexity of the numerical solution, we compare the execution time of both the numerical solution and the analytical solution. Table 2 shows the execution time of both schemes when a dual core 2.66 GHz computer is used as a computational platform. This old desktop computer is 13.33 times faster than the current available on-board computer which is only 200 MHz [25,26]. Table 3 shows a simulated executing time of the on-board flight computer. According to this elapsed time analysis, the proposed 3-dimensional analytical solution has an execution time that is significantly less than that for the fully integrated numerical solution. The analytical solution is more than 140 times faster than the complete numerical solution.

7. Conclusion

In this paper, a full 3-dimensional numerical and analytical solutions are derived for lunar descent and compared in a simulation study. This is the first time in the literature that a complete analytical 3-dimensional solution is derived as compared to the frequently adopted simplifying assumption of a 2-dimensional trajectories. Simulation results show that the numerical and analytical solutions are almost similar except for the altitude. This low altitude flight path of the analytical solution may assist the lunar landing spacecraft to activate terrain based navigation

accessories for hazard avoidance and safe landing. In the proposed scheme, the availability of the descent velocities, time, altitude, down range and cross range as a function of the velocity vector pitch angle can be utilized to reduce the computational burden on real-time lunar descent guidance algorithms for future precise landing missions.

Acknowledgements:

This article was funded by the Deanship of Scientific Research (DSR), King Abdulaziz University, Jeddah. The authors, therefore, acknowledge with thanks DSR technical and financial support. It was also supported by the facility of Japan Aerospace Exploration Agency (JAXA).

Corresponding Author:
Dr. Ibrahim Mustafa Mehedi
Department of ECE
King Abdulaziz University
Jeddah, Saudi Arabia
E-mail: imehedi@kau.edu.sa

References

[1] Cheng RK. Lunar Terminal Guidance. Lunar Missions and Exploration, edited by C. T. Leondes and R. W. Vance, Univ. of California Engineering and Physical Sciences Extension Series, Wiley, New York, 1964. pp. 308-355.

[2] Cheng YH, Meredith CM, and Conrad DA. Design considerations for surveyor guidance. Journal of Spacecraft and Rockets, 1966. 3(11):1569–1576.

[3] McInnes CR. Gravity-turn descent from low circular orbit conditions. Journal of Guidance Control and Dynamics, Jan.-Feb. 2003. 26(1):183–185.

[4] Klumpp RA. Apollo guidance, navigation, and control: Apollo lunar-descent guidance. Technical report, MIT Charles Stark Draper Laboratory, June 1971.

[5] Klumpp RA. Apollo lunar descent guidance, Automatica, 1974. 10(2):133–146.

[6] Ueno S, Yamaguchi Y. Near-minimum guidance law of a lunar landing module. 14thIFACSymposiumonAutomaticControlinAerospace, 1998. 377–382.

[7] Sostaric R. Lunar descent reference trajectory. Technical report, NASA/JSC, March 2006.

[8] Xing-Long L, Gaung-Ren D, Kok-Lay T. Optimal soft landing control for moon lander. Automatica, Feb. 2008. 44: 1097–1103.

[9] Chao B, Wei Z. A guidance and control solution for small lunar probe precise-landing mission. Acta Astronautica, Feb. 2008. 62:44–47.

[10] Braun RD, Manning R.M. Mars exploration entry, descent and landing challenges. Journal of Spacecraft and Rockets, 2007. 44(2):10–323.

[11] Lutz T. Application of auto-rotation for entry, descent and landing on mars. 7thInternational Planetary Probe Workshop, 2010.

[12] Blackmore L, Acikmese B, Scharf D.P. Minimum landing-error powered descent guidance for mars landing using convex optimization. AIAA Journal of Guidance, Control and Dynamics, 2010. 33(4):1161–1171.

[13] Shang Kristian YH, Uldall Kristiansen PL. Dynamic systems approach to the lander descent problem. AIAA Journal of Guidance, Control, and, 2011. 34(3):911–915.

[14] McInnes CR. Direct adaptive control for gravity-turn descent. Journal of Guidance, Control, and Dynamics, Mar-Apr 1999. 22(2):373–375.

[15] Chomel C, Bishop R. Analytical lunar descent guidance algorithm. Journal of Guidance, Control and Dynamics, 2009. 32(3):915–926.

[16] Topcu U, Casoliva J, Mease K.D. Minimum-fuel powered descent for mars pinpoint landing. Journal of Spacecraft and Rockets, 2007. 44(2):324–331.

[17] Najson F, Mease KD. Computationally inexpensive guidance algorithm for fuel-e□cient terminal descent. Journal of Guidance, Control and Dynamics, 2006. 29(4):955–964.

[18] Mattingley J, Boyd S. Real-time convex optimization in signal processing. IEEE Signal Processing Magazine, 2010. 3(11):1569–1576.

[19] Acikmese B, Polen SR. A convex programming approach to constrained powered descent guidance for mars pinpoint landing. AIAA Journal of Guidance, Control and Dynamics, 2007. 30(5):1353–1366.

[20] Sturm JF. Implementation of interior point methods for mixed semidefinite and second order cone optimization problems. Optimization Methods and Software, 2002. 17(6):1105–1154.

[21] Sturm JF. A matlab toolbox for optimization over symmetric cones. Optimization Methods and Software, 1999. 11(1):625–635.

[22] Ye Y. Interior Point Algorithms, volume 33. Wiley, New York, 1997.

[23] Acikmese B, Blackmore L. Lossless convexication for a class of optimal control problems with nonconvex control constraints.

Automatica, 2011. 47(2):341–347.
[24] Steinfeld BA, Grant MJ, Matz DA, Braun RD, Barton GH. Guidance, navigation and control system performance trades for mars pinpoint landing. AIAA Journal of Spacecraft and Rockets, 2010. 47(1).
[25] Nadim F, Haddad RD, Brown, Ferguson R, Andrew T, Kelly T, Reed K. Second generation (200mhz) rad750 microprocessor radiation evaluation. RADECS IEEE Proceedings, 2011. pp. 877–880.
[26] BAE Systems. Rad750 radiation- hardened power pc microprocessor. ELECTRONICS, INTELLIGENCE and SUPPORT, Technical Specifications, 2008.
[27] Mehedi IM, Kubota T. Advanced guidance scheme for lunar descent and landing from orbital speed conditions. Transaction of Japan Society for Aeronautical and Space Sciences, Aug 2011. 54(184):98–105.

1/22/2022